Effects of Non-Covalent Self-Association on the Subcutaneous Absorption of a Therapeutic Peptide

Dean K. Clodfelter,[1] Allen H. Pekar,[1] Dawn M. Rebhun,[1] Kevin A. Destrampe,[1] Henry A. Havel,[1] Sharon R. Myers,[2] and Mark L. Brader[1,3]

Received July 31, 1997; accepted November 7, 1997

Purpose. To utilize an acylated peptide as a model system to investigate the relationships among solution peptide conformation, non-covalent self-association, subcutaneous absorption and bioavailability under pharmaceutically relevant solution formulation conditions.

Methods. CD spectroscopy, FTIR spectroscopy, equilibrium sedimentation, dynamic light scattering, and size exclusion chromatography were employed to characterize the effects of octanoylation on conformation and self-association of the 31 amino acid peptide derivative des-amino-histidine(7) arginine(26) human glucagon-like peptide (7-37)-OH (IP(7)R(26)GLP-1). Hyperglycemic clamp studies were performed to compare the bioavailability, pharmacokinetics, and pharmacodynamics of solution formulations of oct-IP(7)R(26)GLP-1 administered subcutaneously to normal dogs.

Results. Octanoylation of IP(7)R(26)GLP-1 was shown to confer the propensity for a major solvent-induced conformational transition with an accompanying solvent- and temperature-dependent self-association behavior. Formulations were characterized that give rise to remarkably different pharmacodynamics and pharmacokinetics that correlate with distinct peptide conformational and self-association states. These states correspond to: (i) a minimally associated α-helical form (apparent molecular weight = 14 kDa), (ii) a highly associated, predominantly β-sheet form (effective molecular diameter 20 nm), and (iii) an unusually large, micelle-like soluble β-sheet aggregate (effective molecular diameter 50 nm).

Conclusions. Bioavailability and pharmacokinetics of a self-associating peptide can be influenced by aggregate size and the ease of disruption of the non-covalent intermolecular interactions at the subcutaneous site. Hydrophobic aggregation mediated by seemingly innocuous solution formulation conditions can have a dramatic effect on the subcutaneous bioavailability and pharmacokinetics of a therapeutic peptide and in the extreme, can totally preclude its absorption. A size exclusion chromatographic method is identified that distinguishes subcutaneously bioavailable aggregated oct-IP(7)R(26)GLP-1 from non-bioavailable aggregated oct-IP(7)R(26)GLP-1.

KEY WORDS: peptide; aggregation; subcutaneous absorption; glucagon-like peptide-1.

[1] Biopharmaceutical Development, Lilly Research Laboratories, Eli Lilly and Company, Indianapolis, Indiana 46285.

[2] Diabetes Research, Lilly Research Laboratories, Eli Lilly and Company, Indianapolis, Indiana 46285.

[3] To whom correspondence should be addressed. (E-mail: brader_m_1@lilly.com)

ABBREVIATIONS: Glucagon-like peptide-1(7-37)-OH (GLP-1); imidazopropionyl(7) arginine(26) lysine(34)-human glucagon-like peptide-1 (IP(7)R(26)GLP-1); imidazopropionyl(7) arginine(26) N^{ε}-octanoyl-lysine(34)-human glucagon-like peptide-1 (oct-IP(7)R(26)GLP-1); circular dichroism, CD; size exclusion chromatography, SEC; Fourier transform infrared, FTIR; phosphate buffered saline, PBS.

INTRODUCTION

The efficacy of subcutaneously administered therapeutic proteins and peptides is critically dependent upon the absorption and subsequent delivery of the biologically active form of the drug to the site of action. The task of the formulation scientist includes conferring the appropriate shelf-life and in-use stability as well as stabilizing the molecule in a form that facilitates optimal bioavailability and biopotency. The formulation design may also play the principal role in mediating drug absorption thus providing a means to tailor appropriate pharmacokinetics for the drug. Currently, most biopharmaceuticals are administered via subcutaneous injection or intravenous infusion. While the importance of chemical and physical stability are obvious, the potential pharmacological consequences of non-covalent solution structural phenomena such as alternative molecular conformations and/or self-association may be a poorly appreciated but critical aspect of the overall therapeutic success of the drug. This is particularly relevant to discovery and early stage drug development where a large-scale screening strategy or an emphasis on speed-to-first-efficacy-dose may preclude a detailed solution characterization of the molecule prior to dosing (1). The non-covalent aggregation of protein pharmaceuticals is a well recognized problem that has been studied largely in the context of insoluble forms, including precipitates, fibrils, and gels (2,3). These insoluble products have been attributed to the formation of partially unfolded intermediates with an exposed hydrophobic region that drives the aggregation towards the pharmaceutically undesirable form (2–4). Previous studies of this mechanism have been performed by introducing a denaturant to generate the partially unfolded intermediate (4,5). By studying an acylated peptide we have effectively introduced an artificial hydrophobic region to the surface of the peptide in the absence of a denaturant. This approach has facilitated an investigation of the relationship between hydrophobic aggregation and subcutaneous bioavailability under pharmaceutically relevant solution conditions.

Glucagon-like peptide-1(7-37)-OH (GLP-1) is a 31 amino acid hormone liberated by the proteolytic processing of the 160 amino acid precursor protein, preproglucagon. GLP-1 stimulates the secretion of insulin and thus has the ability to normalize blood glucose levels (6). Interest in GLP-1 and its analogs has intensified recently as the attractiveness of GLP-1 as a potential therapeutic agent for the treatment of type II diabetes has been recognized (6–8). The structure of the analog we have studied is shown in Figure 1 and will be abbreviated as oct-IP(7)R(26)GLP-1. This molecule exhibits three changes from the native GLP-1(7-37)-OH structure: the amino group has been removed from the His(7) residue (becoming des-amino-histidine, or imidazopropionyl and is abbreviated herein as IP), Lys(26) has been replaced by Arg, and Lys(34) has been acylated with the straight chain fatty acid octanoic acid (abbreviated as oct). The present study characterizes the effect of the octanoyl acylation on the structure, conformation and self-association of this GLP-1 analog and demonstrates that these properties are highly solvent dependent. This molecule thus affords an opportunity to investigate the relationships among peptide secondary structure, non-covalent molecular association, subcutaneous bioavailability and the pharmacodynamics

of a single therapeutic peptide formulated under different, pharmaceutically typical solution conditions. Of additional significance to this study is the fact that the acylation of proteins *in vivo* is a recently recognized covalent modification involved in intracellular signaling pathways (9). The way in which the acylation mediates these processes is poorly understood. The IP(7)R(26) GLP-1 moiety thus represents a useful model system to investigate the effects of acylation on peptide conformational and associative behavior.

MATERIALS AND METHODS

Materials

Oct-IP(7)R(26)GLP-1 and IP(7)R(26)GLP-1 were provided by Eli Lilly and Company as highly purified lyophilized powders. All other chemicals were of analytical reagent grade. Dulbecco's phosphate buffered saline without Ca and Mg (PBS) was obtained from ICN Biomedical Inc. Solution concentrations of oct-IP(7)R(26)GLP-1 and IP(7)R(26)GLP-1 were calculated based on the respective extinction coefficients of 1.95 $(mg/ml)^{-1} \cdot cm^{-1}$ and 2.01 $(mg/ml)^{-1} \cdot cm^{-1}$ at 279 nm.

Size Exclusion Chromatography

Based on criteria of selectivity and resolution, a 25 cm × 9.4 mm Zorbax GF-250 special column was chosen for the present studies with a mobile phase comprising 14 mM sodium phosphate dibasic adjusted to pH 7.4 with 85% phosphoric acid. The flow rate was 1 ml/min and the injection volume was 50 µl of a 1 mg/ml solution. The eluent was detected using UV absorbance at 214 nm. (Detailed studies to investigate the chromatographic properties of several SEC columns under various mobile phase conditions were undertaken and will be reported elsewhere (10)).

Circular Dichroism Spectroscopy

Circular dichroism spectra were recorded using an AVIV Model 62A DS spectrometer calibrated with (1S)-(+)-10-camphorsulfonic acid. Circular dichroism is reported as mean residue elipticity, $[\theta]_\lambda$, having units of degrees $\cdot cm^2 \cdot dmol^{-1}$. Secondary structural analyses were performed using the program CONTIN (11–12).

Analytical Ultracentrifugation

Sedimentation equilibrium experiments were carried out at 4 °C in a Beckman XLA analytical ultracentrifuge using absorbance optics. Cells with quartz windows and either 3 mm or 12 mm centerpieces were used. The apparent weight-average molecular weights, $M_{w,app}$, were calculated from equation (1).

$$M_{w,app} = \left(RT/\left((1 - \nu\rho)\omega^2 rC\right) \cdot dC/dr \right. \quad (1)$$

where R is the gas constant, T is temperature, ν is the partial specific volume, ρ is the solvent density, r is radius, ω is the angular velocity and C is the total protein concentration in mg/ml. A partial specific volume of 0.726 ml/gram was calculated from the amino acid composition (13). It was assumed that the addition of the acyl group did not change the value of ν. The solvent density was measured using a Paar DMA48 densitometer. Data analyses to model the self-association and determine equilibrium constants (14) were carried out using the program NONLIN, available through the National Analytical Ultracentrifuge Facility at the University of Connecticut. NONLIN gives values of equilibrium constants $k_{1,n}$ on (a mg/ml concentration scale) which refer to the reversible formation of an n-mer from n monomeric units, as described by equation (2). (Thus the tetramer constant $k_{1,4}$ corresponds to the reaction of four monomers to give a tetramer; $k_{1,8}$ corresponds to the reaction of eight monomers to give an octamer; $k_{4,8}$ corresponds to the reaction of two tetramers to give an octamer). The corresponding molar equilibrium constant $K_{1,n}$ is given by equation (3).

$$k_{1,n} = [n - mer]/[monomer]^n \quad (2)$$

$$K_{1,n} = k_{1,n} \cdot (\text{monomer molecular weight})^{n-1}/n \quad (3)$$

Infrared Spectroscopy

Infrared spectra were recorded on a Nicolet Magna 750 Fourier transform infrared spectrophotometer equipped with a Nicolet Nic-Plan infrared microscope. Data were acquired for 128 scans at 4 cm^{-1}. Data acquisition and second derivative analysis were performed with Omnic 3.1 software.

Dynamic Light Scattering

Measurements were performed using a Brookhaven Instruments 9000 autocorrelator and goniometer. All measurements were made with a 400 µm pinhole at a 90° scattering angle using a Lexel Model 3500 argon ion laser set at 488 nm as the scattering source. Sample temperature was maintained at 25°C or 5°C by a Neslab RTE-110 temperature bath. Brookhaven Instruments software was used to calculate the diffusion coefficients of the scattering species from the measured autocorrelation function using the method of cumulants. Diffusion coefficients were converted to mean diameters using the Stokes-Einstein relationship. Values for solution viscosities and refractive indices were assumed to be equal to those of pure water.

In Vivo Testing

Study Design and Animals

GLP-1 is an incretin peptide hormone that stimulates insulin secretion from the β-cell in a glucose dependent manner (6). Hyperglycemic clamp experiments (150 mg/dl) were conducted using chronically cannulated, overnight-fasted, conscious male and female beagle dogs weighing 8–15 kg. Pharmacodynamics were evaluated from the plasma insulin data and pharmacokinetics were determined from blood drug levels. The insulin change and drug level areas under the curve were calculated using the trapezoidal rule. Values are reported as the mean ± the standard error of the mean. Prior to initiation of the study the animals were judged to be healthy by physical examination and laboratory tests. Research adhered to the Principles of Laboratory Animal Care of the NIH.

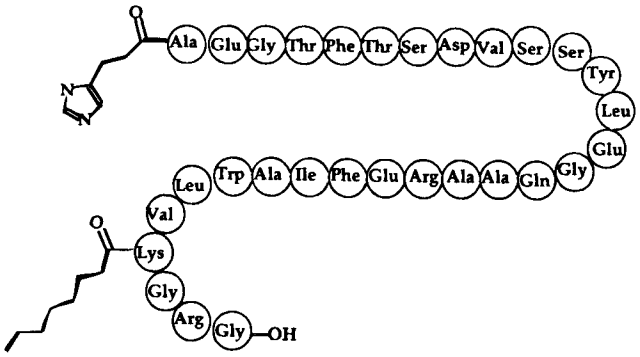

Fig. 1. The structure of imidazopropionyl(7) arginine(26) N^{ε}-octanoyl-lysine(34)-human glucagon-like peptide-1(7-37)-OH (oct-IP(7)R(26) GLP-1).

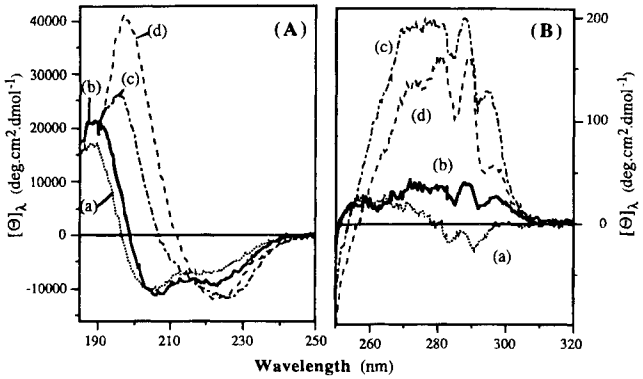

Fig. 2. Panel A: Far-UV CD spectra of IP(7)R(26)GLP-1 (a) and oct-IP(7)R(26)GLP-1 (b) prepared and recorded at 5 °C in 5 mM phosphate buffer, pH 7.5. Oct-IP(7)R(26)GLP-1 prepared and recorded at 5 °C (c) and 22 °C (d) in PBS, pH 7.5. Spectra (a) and (b) were recorded on 0.1 mg/ml and 0.02 mg/ml solutions, respectively. IP(7)R(26)GLP-1 and oct-IP(7)R(26)GLP-1 are monomeric under these conditions. Spectra (c) and (d) were recorded on 0.5 mg/ml solutions. Only minor differences in the CD spectrum of oct-IP(7)R(26) GLP-1 in PBS were apparent over the concentration range 0.1–0.5 mg/ml. Panel B: Near-UV CD spectra of IP(7)R(26)GLP-1 (a) and oct-IP(7)R(26)GLP-1 (b) prepared and recorded at 5 °C in 5 mM phosphate buffer, pH 7.5. Oct-IP(7)R(26)GLP-1 prepared and recorded at 5 °C (c) and 22 °C (d) in PBS, pH 7.5. Spectra were recorded on 0.5 mg/ml solutions.

Formulation Preparation and Administration

Formulations were injected subcutaneously into the dorsal aspect of the neck at a dose of 3 nmol/kg. Four formulations stabilizing distinct conformational and self-association states (*vide infra*) of oct-IP(7)R(26)GLP-1 were evaluated. These formulations were prepared by dissolving lyophilized oct-IP(7)R(26)GLP-1 under the following conditions: (i) 5 mM phosphate buffer, pH = 7.5 prepared at room temperature immediately prior to administration ($M_{w,app}$ approximately 14 kDa by equilibrium sedimentation) (ii) PBS, pH = 7.5 prepared at room temperature immediately prior to administration (quadratic diameter approximately 10 nm by dynamic light scattering at time of dosing) (iii) PBS, pH = 7.5 prepared and stored at 5 °C for 24 hours prior to dosing (quadratic diameter approximately 20 nm by dynamic light scattering at time of dosing), and (iv) PBS, pH = 7.5 prepared and stored at room temperature for 24 hours prior to dosing (quadratic diameter approximately 50 nm by dynamic light scattering at time of dosing).

RESULTS

Circular Dichroism Studies

The far-UV circular dichroism (CD) spectra of IP(7)R(26) GLP-1 and oct-IP(7)R(26)GLP-1 recorded under monomeric conditions in 5 mM phosphate buffer pH 7.5 are presented in Figure 2A (a) and (b) respectively. These spectra show that octanoylation causes a slight perturbation in the far-UV CD of the IP(7)R(26)GLP-1 peptide (Table I). Figure 2A (a) and (b) appear very similar to that reported for native GLP-1 (15) and were found to exhibit analogous concentration dependencies (an intensification with increasing concentration). A comparison of the CD characteristics of each molecule in 5 mM phosphate buffer pH 7.5 and in PBS showed that the IP(7)R(26) GLP-1 molecule possesses closely similar CD spectra in these two solvents, whereas the octanoylated peptide exhibits dramatically different CD spectra. The CD spectrum of Figure 2A (c) corresponds to an oct-IP(7)R(26)GLP-1 solution prepared in PBS at 5 °C. Comparison of this spectrum with Figure 2A (b) shows that a major conformational rearrangement has occurred. The CD spectrum of Figure 2A (d) corresponds to an oct-IP(7)R (26)GLP-1 solution in PBS prepared and recorded at 22 °C. The data of Table I show that under these solution conditions, an almost complete loss of α-helical structure has occurred.

The corresponding near-UV CD spectra are presented in Figure 2B. These data show that under the higher ionic strength conditions (PBS), oct-IP(7)R(26)GLP-1 is characterized by relatively intense CD features with positive maxima in the range 265–295 nm. These results show that the changes in secondary structure evident from Figure 2A are accompanied by major changes in the chromophoric environments of the aromatic residues.

Table I. Secondary Structural Analyses of the CD Spectra of Figure 2A

Peptide	Solvent	Temp./°C	%α-helix	%β-sheet	%remainder
IP(7)R(26)GLP-1	5 mM PB	5	16	40	43
oct-IP(7)R(26)GLP-1	5 mM PB	5	28	31	42
oct-IP(7)R(26)GLP-1	PBS	5	23	16	61
oct-IP(7)R(26)GLP-1	PBS	22	2	36	62

Note: Analyses were performed on 190–240 nm data using the program CONTIN (11,12). PB refers to phosphate buffer pH 7.5 and PBS refers to 10 mM phosphate buffered saline pH 7.5.

Equilibrium Sedimentation Studies

Detailed analytical ultracentrifugation experiments were performed on IP(7)R(26)GLP-1 and oct-IP(7)R(26)GLP-1 under low ionic strength conditions. In 5 mM phosphate buffer pH 7.5 at 4 °C, the non-acylated compound reached equilibrium in about 25 hours. For the acylated derivative, it was noted that a very slight loss of material occurred with time, possibly due to the slow formation of a small fraction of highly aggregated species. On the assumption that the acylated molecule was close to equilibrium, the apparent weight average molecular weights were calculated and plotted against concentration (Figure 3). Each curve was constructed using data from three cells having different loading concentrations. Overlap of these data was good for each molecule, consistent with self-association. Since native GLP-1(7-37) has been reported to self-associate to tetramers (16), an ideal monomer-tetramer-octamer self-association model was chosen. A good fit of concentration versus radius was achieved with this model for all three cells for IP(7)R(26)GLP-1 and is shown in Figure 3. For the acylated derivative, the monomer-tetramer-octamer model fit the data well in the lower concentration region but not at higher concentrations. However, by including a non-ideality term in the modeling, it was possible to achieve a good fit of these data to a monomer-tetramer-octamer association mechanism. The molar equilibrium constants obtained from the curve fit to the IP(7)R(26)GLP-1 data of Figure 3 were $K_{1,4} = 6.44 \times 10^{11}$, $K_{1,8} = 8.18 \times 10^{27}$ and $K_{4,8} = 1.97 \times 10^{4}$, where $K_{1,4}$ and $K_{1,8}$ correspond respectively to the formation of tetramers and octamers from monomers and $K_{4,8}$ corresponds to the formation of octamers from tetramers. For oct-IP(7)R(26)GLP-1 the values were $K_{1,4} = 7.29 \times 10^{14}$, $K_{1,8} = 4.00 \times 10^{33}$ and $K_{4,8} = 7.53 \times 10^{3}$. These models generated good fits to the experimental data (Figure 3), although we note that they may not necessarily represent unique fits. The larger value of $K_{1,4}$ for the acylated derivative is consistent with the greater concentration dependence of weight average molecular weight over the 0–0.5 mg/ml concentration range. However, the subsequent formation of octamers from tetramers is somewhat smaller for the acylated compound than for the non-acylated compound.

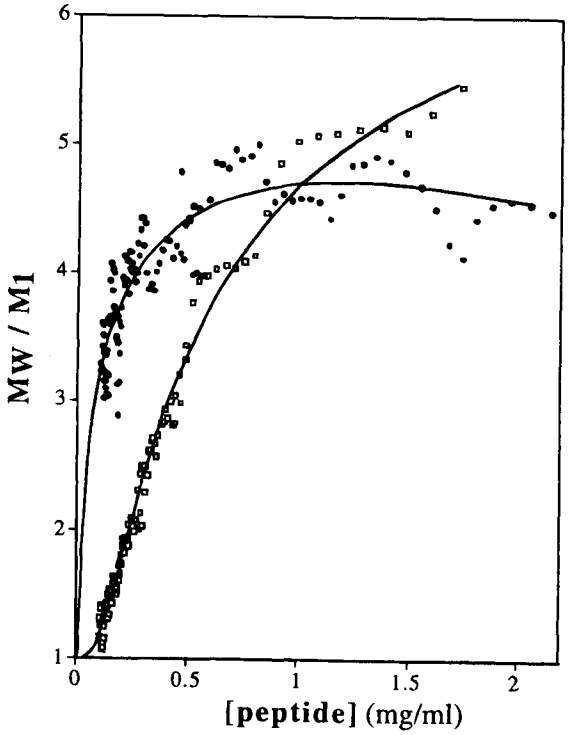

Fig. 3. Equilibrium sedimentation data for IP(7)R(26)GLP-1 (open symbols) and oct-IP(7)R(26)GLP-1 (solid symbols) in 5 mM phosphate buffer pH = 7.5, 4 °C. The solid curves were calculated for a monomer-tetramer-octamer self-association mechanism using the program NONLIN. M_w/M_1 represents the weight average molecular weight obtained from ultracentrifugation divided by the molecular weight of monomer.

Dynamic Light Scattering

In view of the extreme degree of aggregation of oct-IP(7)R(26)GLP-1 in PBS, dynamic light scattering was selected as the most appropriate technique to characterize self-association under these solution conditions. The time-dependence of the aggregation of oct-IP(7)R(26)GLP-1 in PBS at 25 °C and 5 °C as monitored by dynamic light scattering is shown in Figure 4 (a) and (b) respectively. These data show that upon initial reconstitution of the lyophilized powder in PBS at 5 °C, the quadratic diameter is approximately 10 nm. This value increases to about 20 nm over a period of 24 hours. In contrast, for the reconstitution in PBS at 25 °C, the initial quadratic diameter is approximately 20 nm. This value increases to about 50 nm over a period of 24 hours.

Size Exclusion Chromatography

The solvent-dependent CD spectral characteristics of oct-IP(7)R(26)GLP-1 were found to be accompanied by a distinctive size exclusion chromatographic (SEC) signature. The SEC

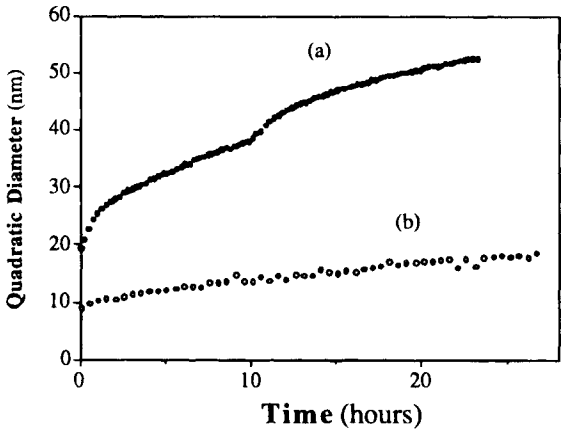

Fig. 4. Dynamic light scattering data for a 0.5 mg/ml solution of oct-IP(7)R(26)GLP-1 formulated in PBS at 25 °C (a) and 5 °C (b). These data show the time dependence of the aggregation of oct-IP(7)R(26)GLP-1 under these solution conditions. The aggregation states shown by dataset (a) at t = 0 and t = 24 hours correspond to those of the samples administered in the dog studies of Figure 7 A and B (b) and Figure 7 C and D (c), respectively. The aggregation state shown by dataset (b) at t = 24 hours corresponds to that of the PBS sample administered in the dog study of Figure 7 C and D (b).

profiles of IP(7)R(26)GLP-1 and oct-IP(7)R(26)GLP-1 prepared in 5 mM phosphate buffer pH 7.5 are presented in Figure 5 (a) and (b) respectively. SEC profiles (c) and (d) correspond to oct-IP(7)R(26)GLP-1 solutions prepared in PBS at 5 °C and 22 °C respectively, and aged at these temperatures for 24 hours prior to analysis. These data show that the SEC retention times of oct-IP(7)R(26)GLP-1 solutions prepared in 5 mM phosphate buffer at 5 °C and in PBS at 5 °C are equivalent. However, in PBS at 22 °C the SEC retention time of oct-IP(7)R(26)GLP-1 is dramatically different and indicative of a much higher apparent molecular weight. It was determined that this aggregated species could be disaggregated in solution by incorporating 30% acetonitrile into the PBS solvent. SEC analysis of this sample (Figure 5 (e)) produced an SEC retention time equal to that of Figure 5 (b). This result indicates that the species corresponding to the SEC peak in Figure 5 (d) is a hydrophobically associated soluble aggregate. The broadness of the oct-IP(7)R (26)GLP-1 peak in (b)–(e) is probably due to enhanced hydrophobic interactions between the peptide and the column packing in addition to on-column equilibria involving a range of aggregation states (17). The chromatograms of Figure 5 (b) and (c) exhibit the same retention time, however, the dynamic light scattering and equilibrium sedimentation data presented herein show that these samples correspond to different states of self-association. The difference between these two aggregation states is not evident by this SEC method, thus it is inferred that the SEC column conditions disrupt the non covalent self-association that occurs in PBS at 5 °C. In contrast, the SEC characteristics suggest a different entity in PBS at 22 °C, an interpretation in accord with the dynamic light scattering data of Figure 4 and the distinctive CD spectroscopic characteristics. Evidently, the peptide molecules are more strongly self-associated in PBS at 22 °C than under the solution conditions of Figure 5 (a)–(c). It is speculated that this aggregate corresponds to a micellar species for which the different CD and SEC characteristics in PBS at 5 °C versus 22 °C, correspond to temperatures that bracket the critical micelle temperature.

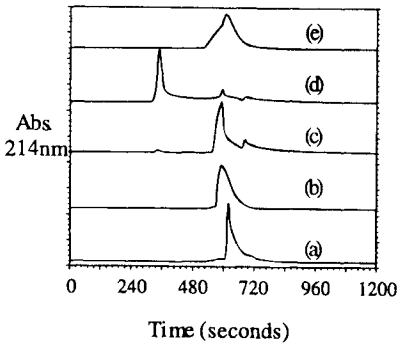

Fig. 5. Size exclusion chromatograms recorded on IP(7)R(26)GLP-1 (a) and oct-IP(7)R(26)GLP-1 (b) solutions prepared at 5 °C in 5 mM phosphate buffer, pH = 7.5. Chromatograms (c) and (d) were recorded on oct-IP(7)R(26)GLP-1 solutions prepared in PBS at 5 °C and 22 °C respectively, and aged at these temperatures for 24 hours prior to analysis. Chromatogram (e) corresponds to a solution of oct-IP(7)R(26)GLP-1 prepared in an identical manner to (d) that had 30% acetonitrile incorporated into the sample solvent immediately prior to SEC analysis. All samples were prepared at a peptide concentration of 1 mg/ml.

Infrared Spectroscopy

Infrared spectroscopy provides a convenient method to probe protein conformation and structure in the solid state. The infrared spectral profiles of the amide region of oct-IP(7)R (26)GLP-1 are presented in Figure 6. Spectrum (A) corresponds to oct-IP(7)R(26)GLP-1, lyophilized from 5 mM phosphate buffer pH 7.5. This spectrum exhibits amide I and amide II bands at 1659 cm^{-1} and 1542 cm^{-1} respectively, values consistent with an appreciable α-helical secondary structure content (18). Spectra (B) and (C) correspond to samples of oct-IP(7)R (26)GLP-1 each lyophilized from PBS, pH 7.5, that had been aged 24 hours at 5 °C and 22 °C respectively. Spectra (B) and (C) both exhibit features at 1695 cm^{-1} (shoulder) 1660 cm^{-1} (main) and 1625 cm^{-1} (shoulder), resolved in the second derivative spectra (not shown). By comparison to spectrum (A) these spectra show that a major conformational change has taken place as a result of dissolving oct-IP(7)R(26)GLP-1 in PBS prior to lyophilization. The IR spectral profiles of (B) and (C) are consistent with a significant increase in β-sheet content (18). The data of Figure 6 establish that in the solid state the oct-IP(7)R(26)GLP-1 species can adopt a secondary structure that is either predominantly α-helical or predominantly β-sheet depending upon the solution conditions from which it was lyophilized. These infrared results on the solid state are in conformity with the CD data for oct-IP(7)R(26)GLP-1 in solution.

In Vivo Testing

The data of Figure 7 compare the plasma insulin responses (A and C) and the plasma drug levels (B and D) for oct-

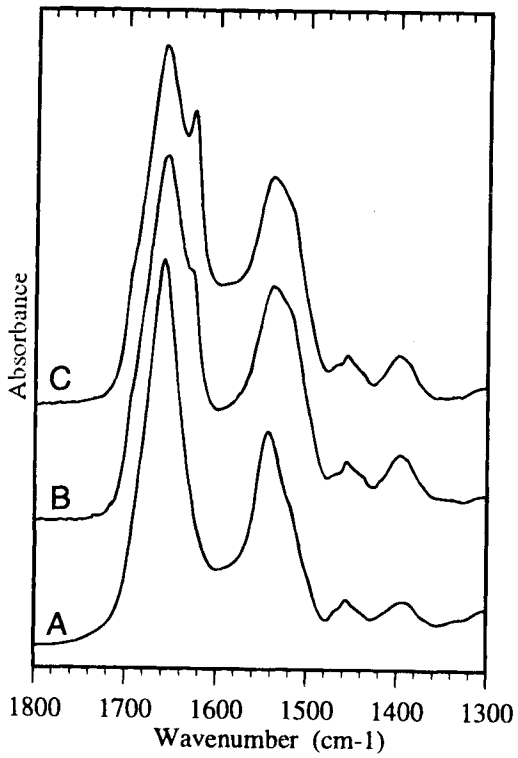

Fig. 6. FTIR spectra recorded on solid samples of oct-IP(7)R (26)GLP-1 prepared by lyophilization from the following solutions; (A) 5 mM phosphate buffer, pH 7.5, T = 5 °C (B) PBS, pH 7.5, T = 5 °C (C) PBS, pH 7.5, T = 22°C.

DOCKET ALARM

Explore Litigation Insights

Docket Alarm provides insights to develop a more informed litigation strategy and the peace of mind of knowing you're on top of things.

Real-Time Litigation Alerts

Keep your litigation team up-to-date with **real-time alerts** and advanced team management tools built for the enterprise, all while greatly reducing PACER spend.

Our comprehensive service means we can handle Federal, State, and Administrative courts across the country.

Advanced Docket Research

With over 230 million records, Docket Alarm's cloud-native docket research platform finds what other services can't. Coverage includes Federal, State, plus PTAB, TTAB, ITC and NLRB decisions, all in one place.

Identify arguments that have been successful in the past with full text, pinpoint searching. Link to case law cited within any court document via Fastcase.

Analytics At Your Fingertips

Learn what happened the last time a particular judge, opposing counsel or company faced cases similar to yours.

Advanced out-of-the-box PTAB and TTAB analytics are always at your fingertips.

API

Docket Alarm offers a powerful API (application programming interface) to developers that want to integrate case filings into their apps.

LAW FIRMS
Build custom dashboards for your attorneys and clients with live data direct from the court.

Automate many repetitive legal tasks like conflict checks, document management, and marketing.

FINANCIAL INSTITUTIONS
Litigation and bankruptcy checks for companies and debtors.

E-DISCOVERY AND LEGAL VENDORS
Sync your system to PACER to automate legal marketing.